Mathematical Biosciences and Engineering

MBE, 19(3): 2355–2380.
DOI: 10.3934/mbe.2022109
Received: 14 October 2021
Revised: 22 November 2021
Accepted: 09 December 2021
Published: 04 January 2022

http://www.aimspress.com/journal/MBE

Research article

Exploring S-shape curves and heterogeneity effects of rumor spreading in online collective actions

Peng Lu[1, 2], Rong He[1] and Dianhan Chen[2,*]

[1] School of Economics and Management, Shananxi University of Science and Technology, Xi'an, China
[2] School of Public Administration, Central South University, Changsha, China

*** Correspondence:** E-mail: sociophysics@hotmail.com.

Abstract: Nowadays online collective actions are pervasive, such as the rumor spreading on the Internet. The observed curves take on the S-shape, and we focus on evolutionary dynamics for S- shape curves of online rumor spreading. For agents, key factors, such as internal aspects, external aspects, and hearing frequency jointly determine whether to spread it. Agent-based modeling is applied to capture micro-level mechanism of this S-shape curve. We have three findings: (a) Standard S-shape curves of spreading can be obtained if each agent has the zero threshold; (b) Under zero-mean thresholds, as heterogeneity (SD) grows from zero, S-shape curves with longer right tails can be obtained. Generally speaking, stronger heterogeneity comes up with a longer duration; and (c) Under positive mean thresholds, the spreading curve is two-staged, with a linear stage (first) and nonlinear stage (second), but not standard S-shape curves either. From homogeneity to heterogeneity, the spreading S-shaped curves have longer right tail as the heterogeneity grows. For the spreading duration, stronger heterogeneity usually brings a shorter duration. The effects of heterogeneity on spreading curves depend on different situations. Under both zero and positive-mean thresholds, heterogeneity leads to S-shape curves. Hence, heterogeneity enhances the spreading with thresholds, but it may postpone the spreading process with homogeneous thresholds.

Keywords: heterogeneity; rumor; spreading; S-shape curves; thresholds

1. Introduction

Nowadays online collective actions, such as rumors spreading on the Internet, become pervasive worldwide, especially on social media Apps, such as Facebook, Twitter, Weibo and WeChat [1−8]. Information attractiveness, rumor propagation, individual judgments, social trust on media, and spreading probability may induce people or agents to believe and spread rumors in cyberspace [4,6,9,10−12]. Rumor spreading has a long story since the beginning of human society [13−18]. For ancient world, rumor spreading strategies have been widely applied to launch protesting, social crisis, natural disasters, or uprisings [19−21]. As an important social phenomenon, rumor spreading can undermine or attack opponents and lead to social panic and destabilization [19,22−24]. The effect of a second rumor counteracting the original rumor also complicates the rumor spreading phenomenon and the mathematical model [25]. Therefore, it is important and necessary to explore the spreading mechanism of rumors or information. For now, more attention has been paid to reasons of online cases, but less has been paid to speading curves, and here we focus the curve shapes of online rumor spreading, for various scenarios.

As a typical category, rumor spreading can be investigated under the perspective of collective actions, which have been explored by social sciences [2−4,9,10,26,27], natural sciences [1,28−32] and other interdisciplinary fields [11,33−37]. For the mechanism of rumor spreading, there are a lot of related models [1−6,8,12,18,38,39−66], and the SIR model is probably the most fundamental and widely used. This model refers to dynamic process of susceptible-infected-removed for individuals [6−8,17,35,39], which was initially applied in epidemics [44−46,48,49,52,54,65]. Then, expanded SIR models are proposed, such as SIS [7], 2SI2R [67], ICSAR [12], SIHR [39], BBV [42], SEIR [44], SIRaRu [45], SICR [46], SSIC [48], DSIR, C-DSIR [57] and ISR [58], etc. They adjust SIR models according to different situations [7,12,39,42,43,45,57,67]. Besides of related SIR models, other methods of ANFIS model [68], Markov chain [31], Lyapunov model [11], machine learning [66], random differential equation (RDE) [35], theory analysis [3,26,37,38,67,69], game theory [11,13,47,66], agent-based modeling [1,9,11,17,29,32,27,33−35,38] and social networks [22,26−29,32,34,35,39,53,55,58,64−67] are also applied and combined to explore the mechanism.

Besides of the spreading mechanism, evolutionary curves (trends) of online collective actions have become critical and remains unsolved [1,3,6,10,15,19,21,24,27,28,37,63,66]. Here, we try to find and verify the mechanisms that generate different curve shapes. As indicated, the common curve shape of collective behaviors (rumor spreading or cooperative actions) is the S-shape [4,6,10,15,19,21,24,27,28,37]. With specific rules and regulations, this is an ideal shape [70−74]. The most ideal type is standard S-shape curve, which is close to accumulative probability curve of the normal distributions [72,74,75], and its density function can be obtained across the whole range. If the function of S-shape curves can be obtained, we are able to predict the whole spreading process of online rumors, in advance. Hence, it is feasible to use it to solve and predict dynamics of spreading curves. In this work, we apply the method of agent-based modeling [1,4,9,11,15,17,21,24,29,32,33,34,35,76], to explore spreading mechanisms of online rumors. Under big data dissemination, mechanism design is critical in determining, investigating, and predicting evolutionary dynamics of online rumors spreading [4,5,7,8,13,26,48,58]. For all the agents, attributions of internal (subjective) thresholds and external social trust thresholds are proposed.

According to real cases observed, both internal and external factors are heterogeneities. To explore different spreading curves of simulations, local neighborhood interactions between agents and their neighbors will be modeled and simulated repeatedly. Based on agent-based modeling, we explore factors and mechanmisms of the rumor spreading process [11,12,18,29,30,33,34,56] or curve shapes [62,66,67,70,71,73−76]. Besides, the rumor spreading is heavily investigated in complex networks [77−94], but little studied applying deterministic models [25].

In the real world, we have different variables or factors that lead to distinct spreading curves. Different parameter settings produce different spreading shapes or curves[1,3,6,17,18,69]. So, we explore the laws and regularities of spreading curves under different conditions. We try to find the best parameter combination, which best fits and explains the spreading curves observed. This paper has five sections. After the introduction section, we propose the modeling and parameter settings in the second section. Then, we report different shapes of curves and dynamic trends. The spreading duration is also observed, and we compare durations under different conditions and situations.

2. Materials and methods

Agent-based modeling and related simulations have become the mainstream modeling pathway to explore the spreading mechanism of information [1,3,6,9,11,12,17,27,29,32−35,38]. For all agents, they should automatically makes decisions by themselves, under specific and dynamic situations or environments. Their actions or behaviors are determined or shaped by certain action rules and individual attributions [3,6,9,11−13,17,27,32,35,36,41,43]. When hearing the rumors, each agent has 3 scoring mechanisms, whose overall thresholds should be satisfied by the times heard.

(a) Internal scoring threshold. Facing the rumors, people online are subjective to internal factors. They will judge or evaluate this information, and decide whether to spread them or not. The internal scoring threshold ($\mathrm{Internal_i}$) refers to the subjective judgement or scoring when hearing the rumors. According to the threshold theory [76], action will happen as long as the threshold can be satisfied or overcome. This internal threshold implies that information (rumor) should satisfy this condition, before it can be spread further. Therefore, the internal threshold denotes the propensity to cut the spreading of rumors. Hence, a higher value of $\mathrm{Internal_i}$ leads to a lower probability of spreading, within minds of agents. This internal scoring threshold is within the mind of individuals, and it is therefore heterogeneous within individuals. This can be also deemed as subjective judgments or attitudes of individuals [9,27]. For instance, thinking the rumor (information) should be known to more, the current agents may tend to spread it, and their internal scoring threshold is much lower. The negative values of $\mathrm{Internal_i}$ implies that the agent will spread romors when first heard them, this is equivalent to the effect of $\mathrm{Internal_i} = 0$.

(b) External scoring threshold. Under certain societies, the external scoring threshold ($\mathrm{External_i}$) refers to general environment (social trust level) that shapes the propensity of spreading for agents. It reflects the macro-level social trust within the society, where agents are interacting with each other and make decisions on spreading. In reality, people are heterogeneous and we apply heterogeneity settings in the Agent-based Modeling [2,3,7,9,11,26,27,30,37]. The $\mathrm{mean}\ (\mathrm{External_i})$ measure the general or aggregate level of social trust. Social trust mechanism [5,9,12,27,28,37,39,43,44,60,61,65−67,95] greatly shapes the spreading pattern of online rumors. For

a society with a low trust level, the rumor spreading can be very fast, and External_i should be very lower. Under a totalitarian and repressive regimes, information is controlled and stratified, and rumors spread pervasively [10,37,96,97]. In a society where we have higher social trust levels, it is difficult to spread rumors and External_i should be larger. When social trust level is lower, the rumor is more likely to be spread. Negative value of External_i implies that the society is running without social trust, this is equivalent to the effect of $\text{External}_i = 0$.

(c) Spreading distances and the combined threshold. The mechanism of threshold and rumor or information spreading can be illustrated in Figure 1, where the Source (in the center) is the initial agent that is spreading the rumors to neighbors. The coordinate of the initial Source is $(0, 0)$, and the coordinate of each agent i is (x, y). For other agent (x, y), the distance to Source is calculate as $\sqrt{(x-0)^2+(y-0)^2} = \sqrt{x^2+y^2}$. The Distance_i refers to total length of the spreading chains, and this length influences agents on whether to spread rumors or not. Besides, the Distance_i also indicates the social distance between the Source to agents. For instance, if the distance is longer, the spreading of rumor (information) becomes weaker, because the rumor has been spread many times before it reaches this agent. If the distance is shorter, the information (rumor) keeps more of original states and seems to be more trustable.

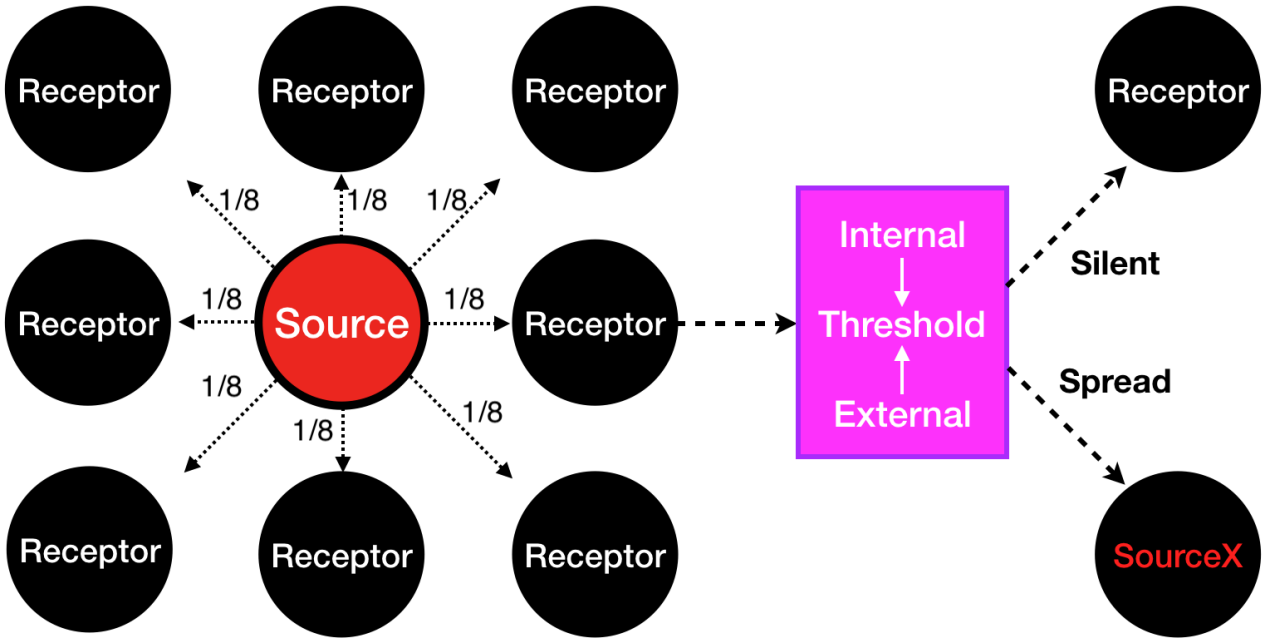

Figure1. Agent-based modeling of rumor spreading mechanism. The red "Source" is the original source, i.e., the first who spread the rumor. SourceX in red refers to the agent who was a receptor before and decided to spread the rumor then.

（d） The hearing times should satisfy combined threshold. In Eq (2.1), the combined threshold (Threshold_i) of each agent (i) is the product of three single or separate threshold mechanisms, such as Internal_i, External_i and Distance_i to the initial Source. Agents may not spread the rumor when first heardring it, but they may do so after hearing the rumor repeatedly. Hence, we apply the parameter $\text{Times. Heard}_i(t)$ to record how many times the agent has heard the rumor. As in Eq (2.2),

it is increased by either one (hearing) or zero (not hearing), at each time. For each agent, the $\mathrm{Times.Heard_i(t)}$ should overcome the ($\mathrm{Threshold_i}$), so that the agent can overcome it and spread the rumor. If not, the agent just hears this rumor, remains silent, and will not spread it. Once the agent i who hears the rumor and decides to spread, its category shifts from the "Receptor" to the "SourceX", which is used to distinguish the initial "Source" in Figure 1.

$$Threshold_i = Internal_i \times External_i \times Distance_i \tag{2.1}$$

$$Times.Heard_i(t) = Times.Heard_i(t-1) + \Delta_t \tag{2.2}$$

$$\Delta_t = \begin{cases} 1 & if\ hearing \\ 0 & no\ hearing \end{cases}$$

(e) Rumor spreading process. Figure 1 depicts the model settings and the spreading process of the rumors, and all agents will interact and spread the rumor on a square lattice. Initially, the original source (in the center) spread the rumors to neighbors randomly. In total, we have two classes of agents (Source or Receptor). For the source, he or she spread the rumors when it begins; for the receptors, they hear (receive) the rumors but merely spread them as their thresholds have been satisfied [6,7,18,27−29,32,39,41,42,45,55,61]. The initial "Source" is set on the center of the world (0, 0), it is the orginal source of the rumor. It spread the rumor randomly to eight neighbors, which implies that each neighbor (receptor) has a 1/8 probability to hear the rumor. For other agents (receptor), the time of hearing the rumor tends to increases, and the spreading threshold of receptors will be overcome gradually. If the threshold of the agent (receptor) is satisfied, it will become a "SourceX", and decide to spread the rumor. We run the simulations and record instant spreading percentage and other observations at each time t. This spreading process goes on until all the agents hear the rumor, i.e., the spreading percentage reaches 100%.

(f) Parameters Settings. All agents stand on the square lattice (size = 51×51). Therefore, the center is (0, 0) and the maximal coordinate of corner agents is (± 25, ± 25). Each agent has eight neighbors to interact with. Considering the heterogeneity of agents, the $\mathrm{Internal_i}$ are subjective and heterogeneous [3,4,5,7,9,11,12,27,32,33,38,39,44]. Both extremely high and low individuals are in a small proportion of the population, and most are in the middle range. Therefore, the distribution of $\mathrm{Internal_i}$ is assumed to be normal distribution. If $\mathrm{Internal_i} = 1$, the internal scoring does not affect the rumor spreading. Similarly, the external scoring threshold ($\mathrm{External_i}$) is assumed to be normally distributed as well. If $\mathrm{External_i} = 1$, it has little influence on the spreading. To reflect these situations, we set their mean values of $\mathrm{Internal_i}$ and $\mathrm{External_i}$ to be one, i.e., $\mathrm{mean(Internal_i)} = \mathrm{mean(External_i)} = 1$. As we plan to compare the effects of threshold, so we also have $\mathrm{mean(Internal_i)} = \mathrm{mean(External_i)} = 0$. For both $\mathrm{Internal_i}$ and $\mathrm{External_i}$, the heterogeneity is determined by SD (standard deviations), $\mathrm{sd1}$ and $\mathrm{sd2}$. To explore full-scale effects of heterogeneities ($\mathrm{sd1}$ and $\mathrm{sd2}$), the serial number of {0, 0.5, 1, 2, 3} is applied in simulations. The $\mathrm{sd1} = \mathrm{sd2} = 0$ refers to the complete homogeneity; $\mathrm{sd1} = \mathrm{sd2} = 1$ means weak heterogeneity; $\mathrm{sd1} = \mathrm{sd2} = 2$ is strong heterogeneity and $\mathrm{sd1} = \mathrm{sd2} = 3$ refers to extreme heterogeneity. For some simulations, we run them 100 to 300 times, and take the mean (average) values as the stable or reliable outcomes.

3. Results

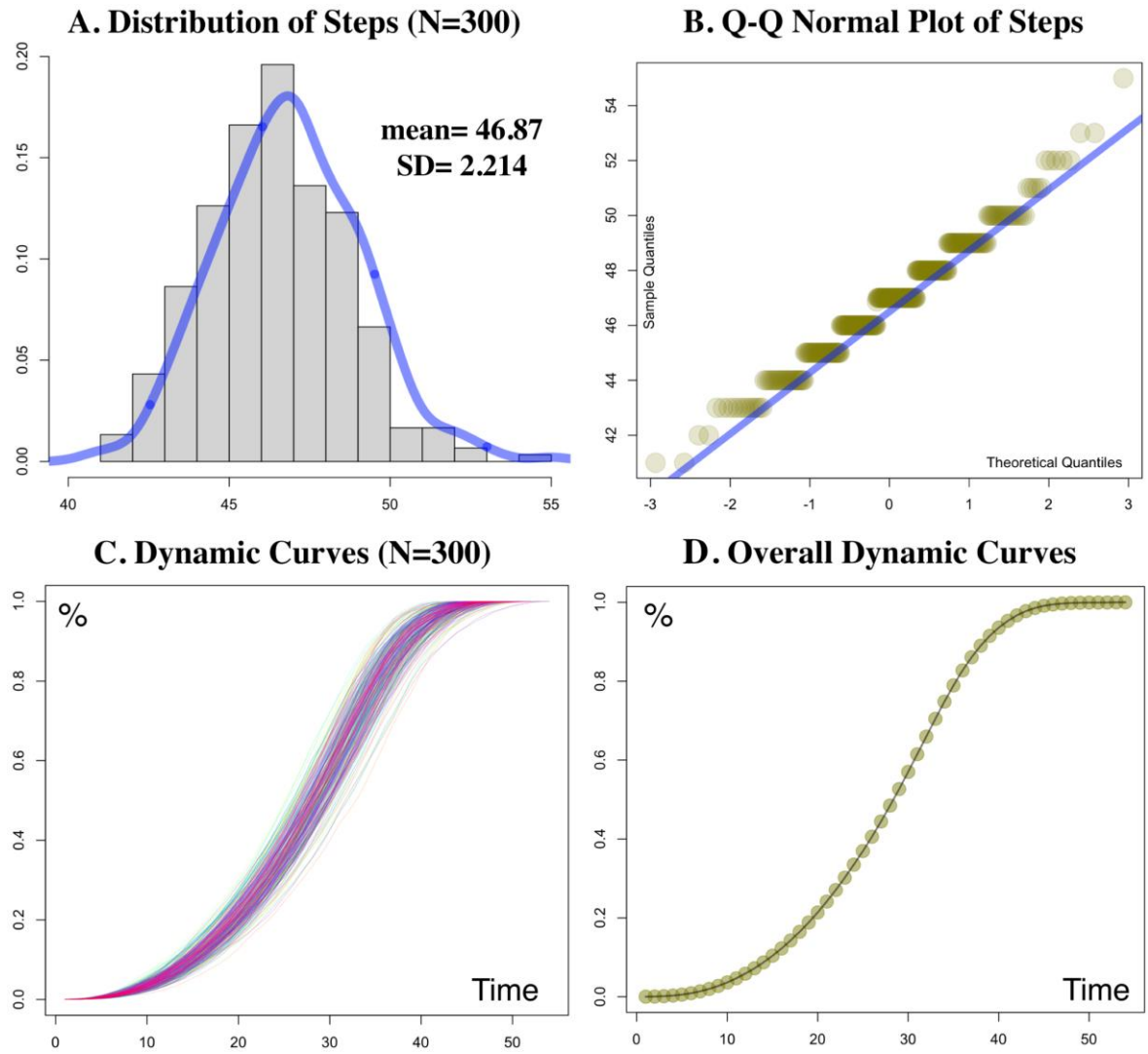

Figure 2. Spreading under homogeneous zero thresholds (ideal state). Subfigure A visualizes the distribution of durations for 300 repeated simulations, and it seems that the average duration (steps) is 46.87. The x-axis is the values of duration, and the y-axis refers to the density; subfigure B checks the normal distribution of the durations (steps). The axis is the theoretical quintiles, and the y-axis refers to the observed sample quintiles. The 300 repeated curves of simulations are visualized in subfigure C, and the overall curves are shown in subfigure D.

We use the software NetLogo 6.1.1 under MacOS system to run model simulations. Netlogo is an multi-agent programming software for simulating complex networks and social phenomena. It is one of the most widely used software for agent-based modeling[98]. Netlogo is especially suitable for modeling complex systems evolving over time [99]. Rumor propagation is a sequential process, so we use netlogo software as our simulation tool. We simulate evolutionary dynamics (curves) of online collective actions, based on variant means and heterogeneities (sd1 & sd2) and other parameter

settings. Hence, the distribution of key variables and curve shapes can be obtained. The exploration ranges from simple situations to complex situations, which aims to better understand and reflect the reality. Here, S-shape curves typically contains three-stages, such as early-stage (slow-growing), middle-stage (fast-growing), and late-stage (slow-growing). For standard S-shape curves, we can see normal distributions of observations. For other S-shape curves that are not standard S-curves, we define them as quasi-S-shape curves, because no normal distributions have been observed.

3.1. Homogeneous zero thresholds

We first explore the simplest situation where there are no thresholds, which are deemed as "homogeneous zero thresholds". The threshold is zero for all agents, i.e., mean and SD of both heterogeneities are zero. For each agent, they will spread the rumor at $(t + 1)$, as long as they hear it in t. Under this case, we obtain the standard S-shape curves. For each rumor spreading process, we observe and record the whole process, in terms of key indicators (variables), such as steps (duration) and the curves. We simulate the model for 300 times, so that we can get their distributions. In Figure 2A, the distribution of steps (durations) can be visualized (N = 300). It seems that it follows the normal distribution as the density line in blue is symmetric and bell-shaped. The longest duration is 54 steps, and the shortest is about 42 steps. The average duration is 46.87 steps and SD is 2.214 steps. We use Q-Q normal plot to check its normal distribution in Figure 2B, and it indicates that most values are normally distributed. In Figure 2C, the 300 curves of rumor spread processes are visualized, and most of them present standard S-shape curves that are symmetric. Each one is similar to the others, and they outbreak and vanish at the same time. For each curve, the spreading percentage grows from zero to 100%. As the 300 spreading curves are generated from the same set of parameters, the average curve of 300 curves is produced to reflect the setting of parameters better than each one of 300 curves. In Figure 2D, the average (overall) curve represents the 300 curves under the homogeneous zero thresholds. Although simple, it provides the baseline of the ideal state where agents spread the rumor as long as they hear or receive it, without difficulties or obstacles (thresholds). Based on this ideal state, we add more real settings or considerations into simulations to explore real-state curves.

3.2. Heterogeneous zero thresholds

Under the "homogeneous zero thresholds" scenario where $\mathrm{sd1} = \mathrm{sd2} = 0$, all thresholds are zero, and there is no obstacles or costs (threshold) for agents to spread rumors. However, under the "heterogeneous zero thresholds" scenario, the mean of thresholds is zero but the SD is non-zero, which means the thresholds for individuals are not zero ($\mathrm{sd1} = \mathrm{sd2} > 0$). Similarly, we run each simulation 300 times to obtain 300 curves under the same set of parameter levels or values. Given the mean is zero, we vary both internal and external heterogeneities to explore the effects of individual heterogeneity ($\mathrm{sd1}$) and social heterogeneity ($\mathrm{sd2}$).

(a) For $\mathrm{sd1} = \mathrm{sd2} = 0.5$, we repeatedly run the simulation and obtain the 300 spreading curves, and then visualize the distribution of durations (N = 300). In Figure 3A, the spreading processes under $\mathrm{sd1} = \mathrm{sd2} = 0.5$ are close to the standard S-curves as well. However, it takes a longer time for the spreading percentage to reach the 100% level because the mean duration is 72.34 steps that is larger

than 46.87 under $sd1 = sd2 = 0$ (the ideal state). Under $sd1 = sd2 = 0.5$, the SD of duration is about 4.23. The distribution of durations is close to the normal distribution as well, because the density line in blue is symmetric.

(b) For $sd1 = sd2 = 1$, the degree of heterogeneities grows further. It seems that the S-shape curves are obvious as well. The distribution of duration is also close to the normal distribution, as the density line is smooth and symmetric. Comparing $sd1 = sd2 = 0.5$ and $sd1 = sd2 = 1$, the curves are more diverse and the spreading duration increases further in Figure 3B. As the heterogeneity grows, it takes longer to achieve the spreading rate of 100%. The average duration is about 102.98 steps, larger than 72.34 steps. The SD is 7.437, larger than 4.23. Besides, the curve starts to have a longer tail under $sd1 = sd2 = 1$.

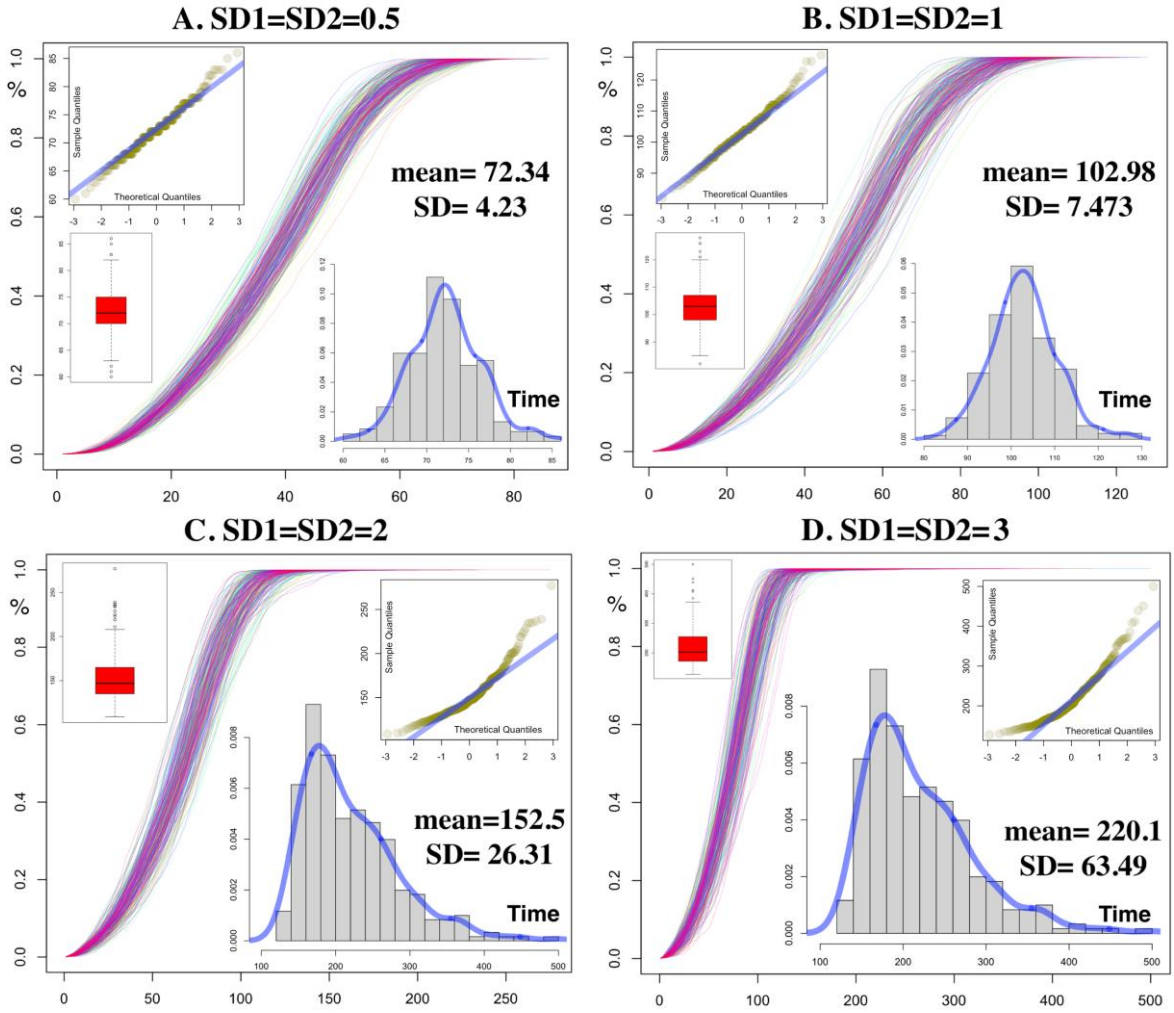

Figure 3. Spreading curves under homogeneous zero thresholds. For all the subfigures, the x-axis is the time (steps) and the y-axis is the accumulative spreading percentage, and we insert the histogram and boxplot, which reflects the distribution of durations, for each subfigure.

(c) For $sd1 = sd2 = 2$, the heterogeneities become much stronger. It seems that standard S-shape curves disappear, but we see quasi-S-shape curves. For each curve, it takes on an S-shape curve first and then with a long straight line. The right tail is more obvious, and it, therefore, takes more time to achieve the 100% spreading percentage. The mean is 152.5, which is much larger than 102.98. For these 300 curves, the tail (if any) usually lasts for 100 steps. This is mainly caused by the increase in heterogeneity. For the distribution in Figure 3C, it does not follow the normal distribution anymore, as the density line in blue is not symmetric or bell-curved. Indeed, the distribution is rather skewed.

(d) Under $sd1 = sd2 = 3$, the heterogeneities are extremely strong. As well, the S-shape curves disappear, and curves are with longer right tails. Their right tails are much more obvious under $sd1 = sd2 = 3$, and it takes a much longer time to achieve 100%. For instance, the average duration is 220.1 steps, which is much larger than 152.5 steps. For these curves, it usually lasts for over 100 steps, which is mainly caused by the growing heterogeneity. The distribution in Figure 3D does not follow the normal distribution anymore, as the density line in blue is not symmetric or bell-curved. The distribution is rather more skewed than $sd1 = sd2 = 2$. The SD is 63.49 steps, which means that curves are much more diverse.

3.3. Curves under thresholds with homogeneity

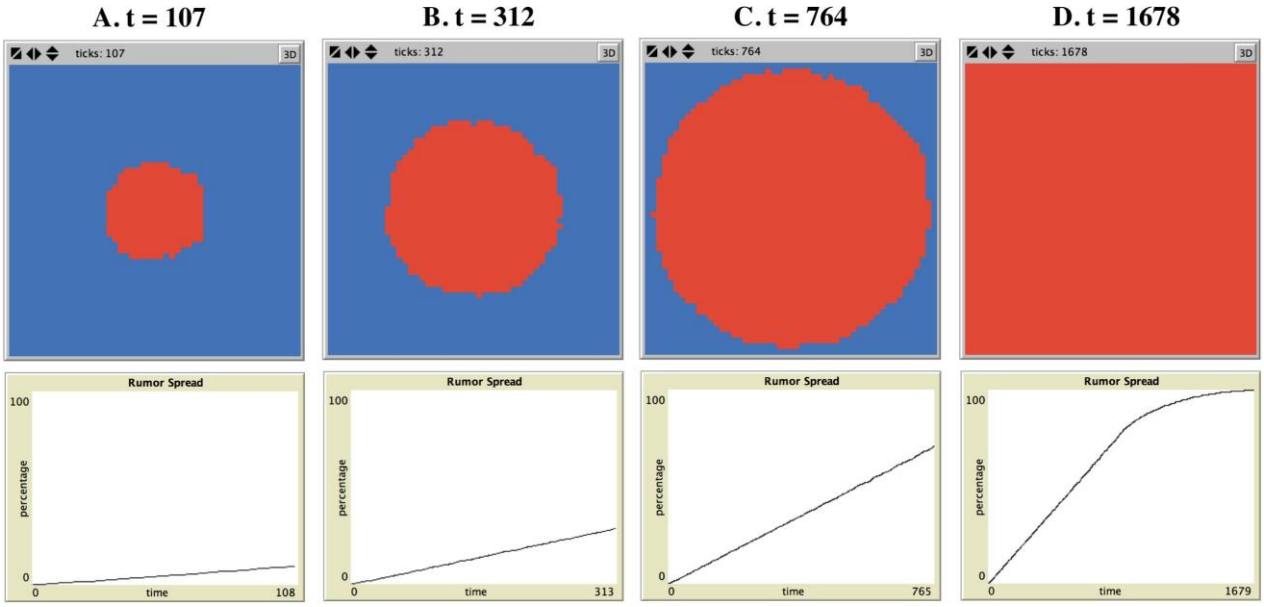

Figure 4. The spreading curve under thresholds with homogeneity. This figure reflects the full process of the rumor spreading under homogeneity. It is obvious that the linear process (first) combines the nonlinear process (then).

Under thresholds with homogeneity, agents have the same thresholds, i.e., $\text{mean}(\text{Internal}_i) = \text{mean}(\text{External}_i) = 1$ and $sd1 = sd2 = 0$. The spreading duration in Figure 4 is relatively time-consuming and it takes over 1600 steps to achieve 100%. Besides, it combines linear and nonlinear stages into a whole process: (a) as t=107, the spreading curve is linear and grows slowly because the spreading of rumors just begins. The percentage in Figure 4A is about 10%; (b) as t = 312, the spreading

curve in Figure 4B is linear as well, and it is around 30%; (c) while t = 746, the curve in Figure 4C is also linear, but the dynamics shift from linear to nonlinear stage. The percentage is about 80%; (d) as t=1678, the spreading process ends and 100% has been achieved. The duration is therefore 1678. The whole curve in Figure 4D has explicit linear and nonlinear stages. In the rapid spreading stage (linear stage), the percentage rate is about 80%; then, it takes a much longer time to reach 100%, in the slowly spreading stage (nonlinear stage).

As it takes a longer time for the spreading to achieve 100%, we merely run it 50 times and obtain 50 spreading curves. Figure 5 visualizes these 50 curves, and they share the same common trends as parameter setting is the same. The common trend (black curve) is calculated as the mean of 50 curves. The turning point D (purple point) can be seen when $t = 900$. The long period of spreading is caused by homogeneity (equal probability). Under homogeneity with threshold, each agent has to accumulate $Times.Heard_i$ to overcome$Threshold_i$. As the probability is 1/8, it is time-consuming for it to spread. The turning point D is mainly caused by the limitation of the available neighborhood. In the earlier period, the number of available neighbors is plenty. However, we have no enough neighbors after the D point. The spreading curves, under thresholds with homogeneity, can explain the reality. For the spreading of breaking news, a much higher spread percentage (for example 80%) can be achieved quickly, at the beginning or outbreak stage. After that, the spreading process slows down. It usually takes a much longer time for it to be known by the whole population. It is even impossible for the 100% spreading percentage can be reached, i.e. the duration of rumor spreading will be definitely long.

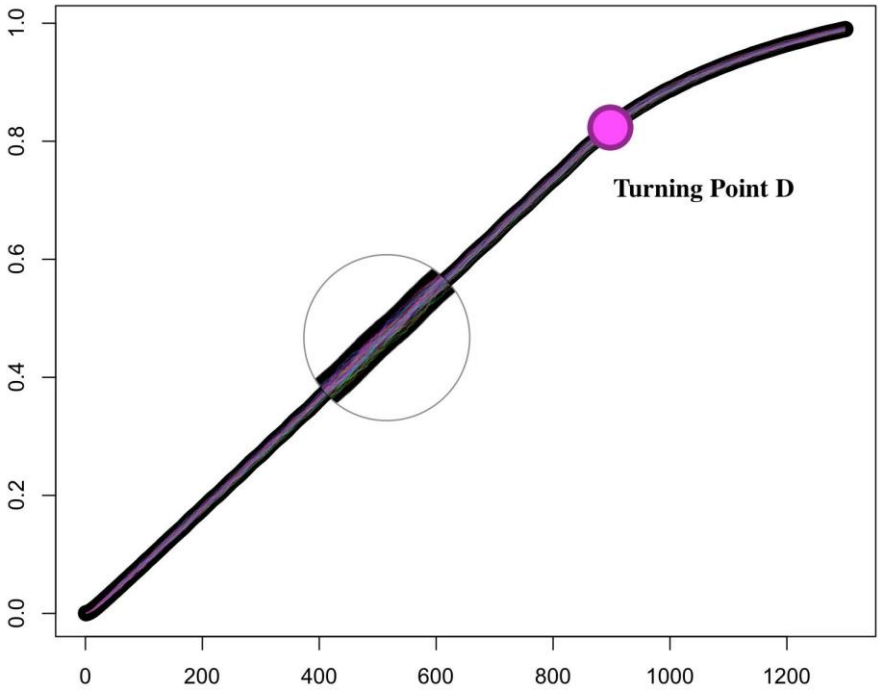

Figure 5. Spreading curves under thresholds with homogeneity (N = 50). It visualizes the overall curves that represent the 50 simulation curves.

3.4. Curves under thresholds with heterogeneity

Figures 4 and 5 visualize the spreading curves under thresholds with homogeneity. It indicates that it is not S-curve but a combination of linear and nonlinear stages. Besides, the spreading process is time-consuming. To compare with "thresholds with homogeneity", here we introduce the "thresholds with heterogeneity" scenario where $sd1 = sd2 > 0$. The agents may have variant thresholds, which are closer to reality. We explore the spreading curves from two aspects: (a) the shape of curves. The spreading curve is more like S-shaped curve. For some cases (breaking news), we also have two-stage curves in Figure 5. There are also observed spreading curves that can be linear combination of the S-shape in Figure 3A,B and two-stage curves in Figure 5; (b) the duration of spreading. The span or duration is another critical indicator. For some cases, the spreading process is completed within a short time; for others, this process takes a long time. Based on previous figures, the heterogeneity may have significant effects on the duration or span. Under thresholds with heterogeneity, it takes a longer time and each simulation is run 100 times.

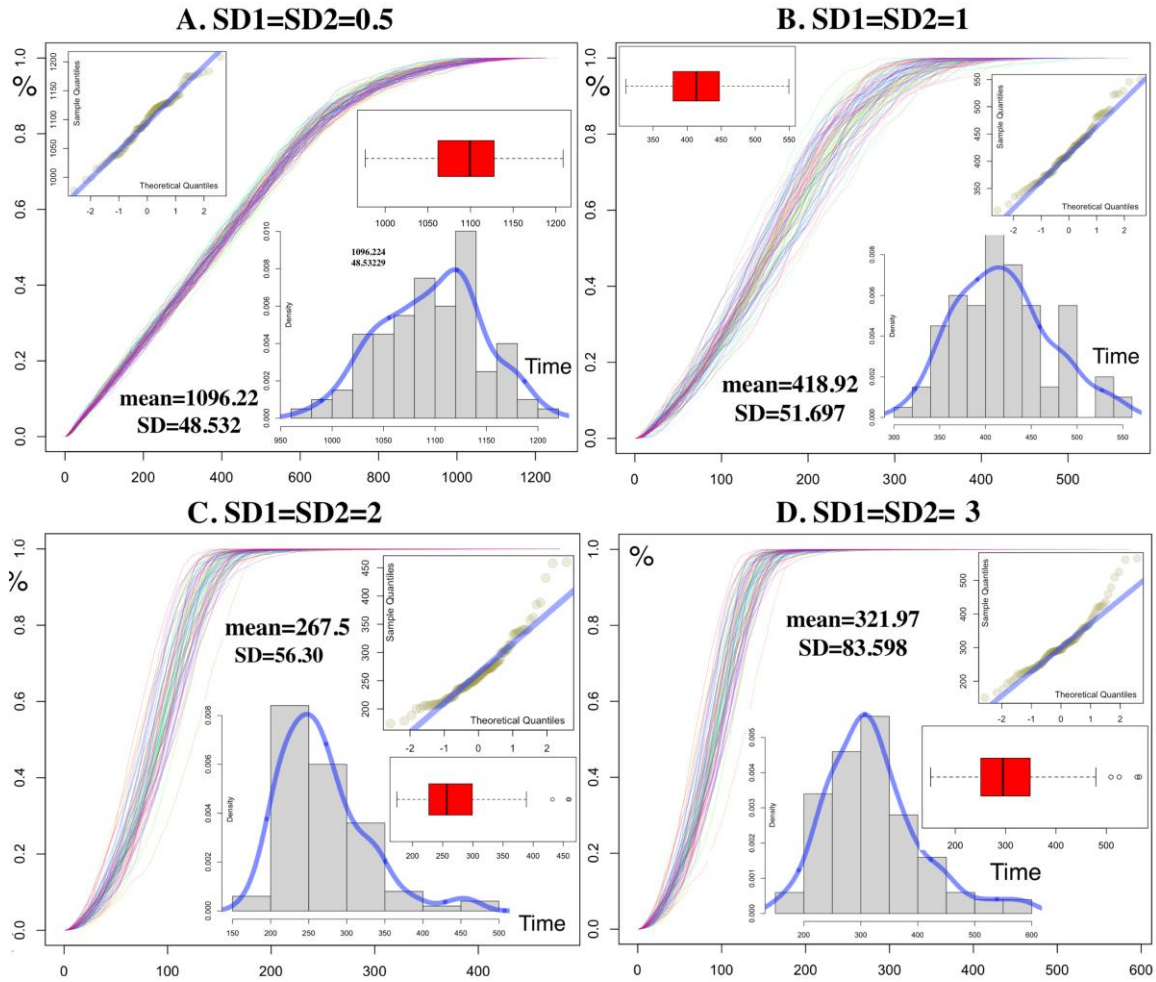

Figure 6. Spreading curves under thresholds with heterogeneity (N = 100). For each subfigure, the 100 simulation curves are depicted, the boxplot in red and histogram in gray are inserted to capture the distribution.

(a) Under $sd1 = sd2 = 0.5$, heterogeneity increases slightly from 0 to 0.5. Figure 6A visualizes evolutionary dynamics curves and distributive traits of durations (N = 100). These spreading curves do not vary a great deal, and they also have two stages, which are similar to Figure 5. The distribution of duration is depicted in Figure 6A, and the distribution is asymmetric but closer to normal distribution. The average duration is slightly reduced as well. The mean is around 1096 steps, less than 1678 in Figure 4. The main reason is that the heterogeneity does not change a lot from homogeneity ($sd1 = sd2 = 0$) and heterogeneity is still weak. Under the weak heterogeneity, the effects are weak as well and the changes are not so obvious.

(b) Under $sd1 = sd2 = 1$. The degree of heterogeneity increases slightly from 0.5 to 1 (middle heterogeneity). There is an obvious variance in spreading curves (N = 100). First, the common trend is stable, and these spreading curves are generally two-staged. It is not enough for this heterogeneity degree to produce the shift of spreading curves. However, the 100 spreading curves are getting more diverse than in Figure 6A, which is mainly caused by the increment of heterogeneity; Meanwhile, the duration of rumor spreading has been largely reduced. Under middle heterogeneity, the mean is 419 steps, much larger than weak heterogeneity (1096 steps), and this is a substantial decrease. It seems that the duration follows the normal distribution, as the density line in blue is smooth and symmetric (bell-curved).

(c) Under $sd1 = sd2 = 2$. The degree of heterogeneity increases from 1 to 2, which is deemed the strong heterogeneity. Some obvious changes can be seen, and the curve shape has been changed, from two-stage curves to S-shape curves. However, this is not the standard S-curve in Figure 3A,B, but the S-curves with longer tails. The strong heterogeneity produces transitions of curves' shape. As well, the 100 spreading curves are getting as diverse as Figure 6B, which is mainly caused by the increment of heterogeneity; Meanwhile, the rumor spreading duration has been reduced further. Under middle heterogeneity, the mean is 419 steps, but it is merely 268 steps under the strong heterogeneity, which is a substantial decline. The duration does not follow normal distribution, as it is obviously skewed.

(d) Under $sd1 = sd2 = 3$, the heterogeneity grows from 2 to 3, which is the extreme heterogeneity. This extreme heterogeneity produces significant changes in terms of the curves' shape (N = 100). Under extreme heterogeneity, it is neither two-staged nor S-shaped, but the S-shape curve with a long tail. They are getting more diverse as well, which is mainly caused by the growing heterogeneity. It has been indicated in Figure 6A-C that heterogeneity reduces the duration of spreading. However, the duration increases slightly under extreme heterogeneity. Under strong heterogeneity, the mean is 268, but 322 steps under extreme heterogeneity. The duration does not follow normal distribution as well, as the density line is obviously skewed. However, heterogeneity generally reduces the duration and facilitates the spreading, which holds true especially within the normal range.

4. Exploring the duration of spreading

Besides spreading curves, we explore the spreading duration. In general, we have two scenarios which are under no thresholds where $\text{mean}(\text{Internal}_i) = \text{mean}(\text{External}_i) = 0$, and under thresholds where $\text{mean}(\text{Internal}_i) = \text{mean}(\text{External}_i) = 1$. For two situations, each heterogeneity (sd_1 or sd_2) takes 21 values from {0, 0.05, 0.1, 0.015, …, 2.95, 3) and we run

simulations to obtain outcome observations, and investigate the relationship between durations and heterogeneities. Eqs (4.1)−(4.3) explore the effects of single heterogeneity (sd_1 or sd_2) and the total heterogeneity SD. As in Figure 6, the effects of heterogeneities may be nonlinear, so we add nonlinear terms SD^2, sd_1^2 and sd_2^2 into Eqs (4.4)−(4.6) to explore quadratic effects. For each, β_0 refers to the constant and ε is the residual. We have two advantages to evaluate the factors and durations of rumor spreading. The first one is that we can back-calculate and predict the trend in advance by doing this. The second is that we can accurately know the effects of related possible factors

$$Duration = \beta_0 + \beta_1 \cdot sd_1 + \beta_2 \cdot sd_2 + \varepsilon \tag{4.1}$$

$$\text{Duration} = \beta_1 \cdot \text{sd}_1 + \beta_2 \cdot \text{sd}_2 + \varepsilon \tag{4.2}$$

$$\text{Duration} = \beta_0 + \beta_1 \cdot \text{SD} + \varepsilon \tag{4.3}$$

$$\text{Duration} = \beta_0 + \beta_1 \cdot \text{SD} + \beta_2 \cdot \text{SD}^2 + \varepsilon \tag{4.4}$$

$$\text{Duration} = \beta_0 + \beta_1 \cdot \text{sd}_1 + \beta_2 \cdot \text{sd}_1^2 + \varepsilon \tag{4.5}$$

$$\text{Duration} = \beta_0 + \beta_1 \cdot \text{sd}_2 + \beta_2 \cdot \text{sd}_2^2 + \varepsilon \tag{4.6}$$

4.1. Under zero thresholds

Table1. Linear and nonlinear effects of heterogeneity under zero thresholds[a].

	Model 1	Model 2	Model 3	Model 4	Model 5	Model 6
C	615.274*** (24.119)	/	/	/	/	/
sd_1	-41.56*** (6.271)	62.44*** (7.505)	/		274.42*** (20.238)	
sd_1^2					-43.96*** (5.102)	
sd_2	-45.09*** (6.271)	58.89*** (7.505)	/			278.26*** (20.319)
sd_2^2						-45.21*** (5.122)
$SD = (sd_1 + sd_2)$			52.29*** (2.749)	139.13*** (10.160)		
$SD^2 = (sd_1 + sd_2)^2$				-11.30*** (1.281)		
F-Statistics	F (2, 438) =47.8***	F (2, 439) =243.6***	F (1, 440) =361.9***	F (2, 439) =251.5***	F (2, 439) =255.3***	F (2, 439) =251.5***
N	441	441	441	441	441	441
Adjusted R^2	0.1754	0.5238	0.45	0.5319	0.5356	0.5319

a. * p < 0.05, ** p < 0.01, *** p < 0.001.

First, we explore the durations under the scenario of zero thresholds. Models 1−6 are correspondence to Eqs (4.1)−(4.6). In model 1, we add the intercept β_0, and it seems that both sd_1 and sd_2 have significant and negative effects on the duration of collective actions. However, the explanatory power (adjusted R^2) is as low as 17.54%. Hence, we drop the intercept β_0 in models 2 to 6. Model 2 suggests that both sd_1 and sd_2 have positive effects on durations, which means that heterogeneity enlarges the spreading duration (process). In model 3, we focus on the aggregate heterogeneity of $\mathrm{SD}= \mathrm{sd}_1 + \mathrm{sd}_2$. It indicates that SD has positive effects on spreading durations as well. The linear effects of heterogeneity can be evaluated by models 1−3. As there exist the nonlinear effects of heterogeneity as well in Figures 5 and 6. We introduce quadratic forms of sd_1, sd_2 and SD to explore linear and nonlinear effects in models 4−6. We estimate the nonlinear effects of SD in model 4 and this nonlinear effect is statistically significant. There is a peak point as the nonlinear effect (quadratic form) is negative. The adjusted R2 is about 53.19%, larger than the linear effect in model 3 (45%). In model 5, we investigate nonlinear effect of sd_1 and the pattern of sd_1 is similar to SD. The coefficient of the quadratic form sd_1^2 is negative, and the coefficient of sd_1 is positive. Hence, there should be a certain sd_1 level that achieves the peak or highest spreading duration. The adjusted R2 in model 5 is higher than the merely linear effect in model 2 (53.56% > 52.38%). We explore nonlinear effect of sd_2 in model 6, and the nonlinear effect of sd_2^2 is negative as well. The heterogeneity postpones the complete (100%) spreading of rumors under zero thresholds.

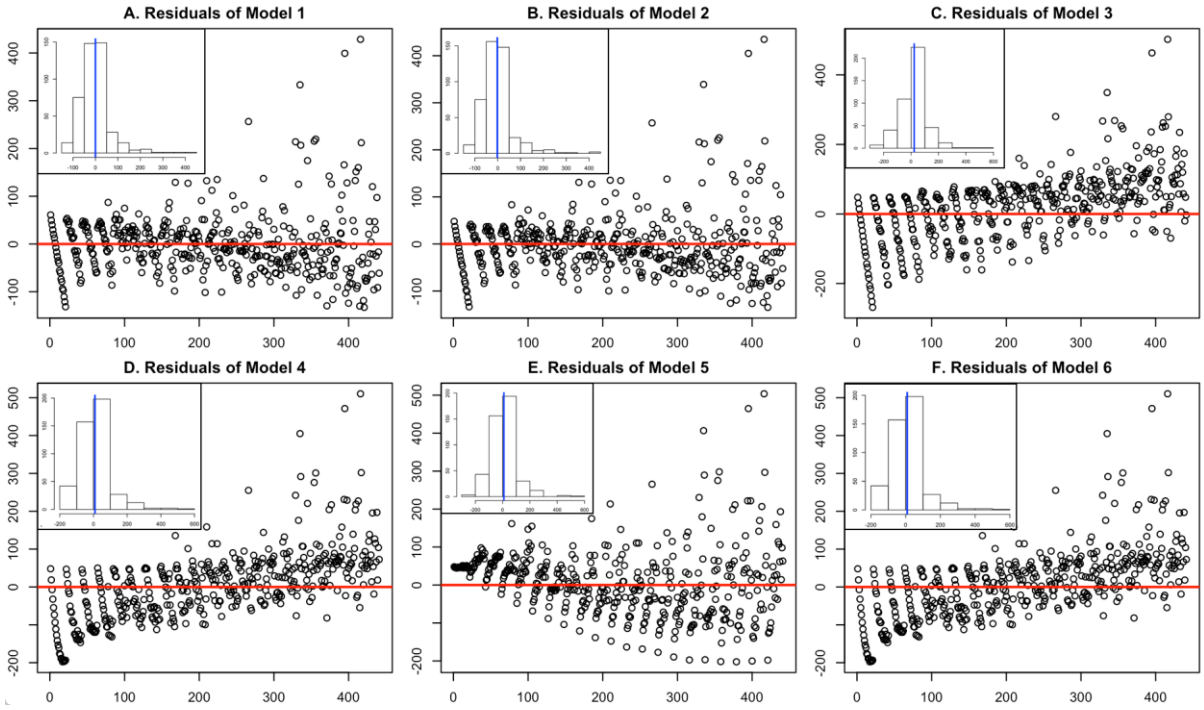

Figure 7. Distributions of residuals for models 1 to 6. It visualizes the values of residuals for models 1−6. For each figure, the histogram is provided as the subfigure, and the vertical blue line refers to the mean values.

In Figure 7, we check the distribution of residuals for models 1−6. It suggests that the means of six residuals (blue vertical lines in the subfigures) are close to zero for most models, although some diverse values can be observed.

4.2. *Under thresholds*

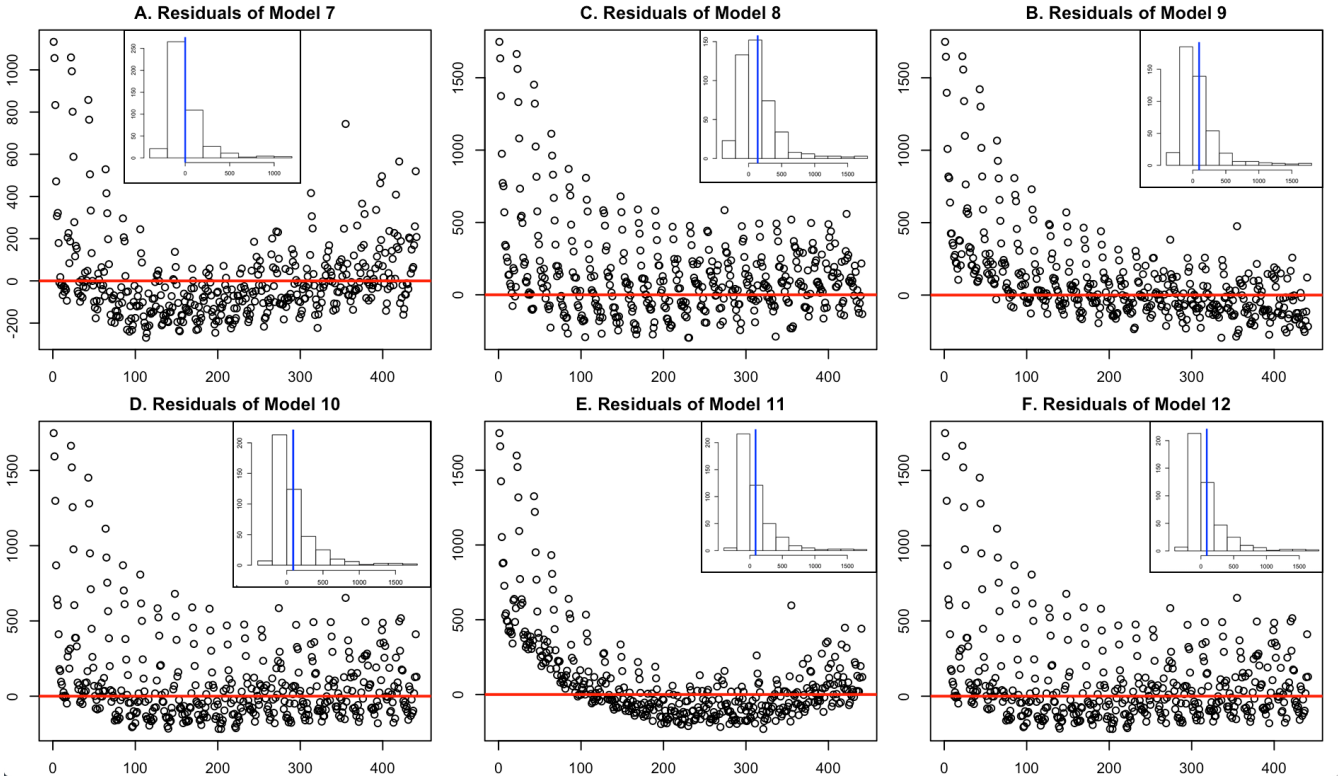

Figure 8. Distributions of residuals for models 7−12. It visualizes the values of residuals for models 7−12. For each figure, the histogram is provided as the subfigure, and the vertical blue line refers to the mean values.

Then, we explore durations under thresholds where $\text{mean}(\text{Internal}_i) = \text{mean}(\text{External}_i) = 1$ and $\text{sd}_1/\text{sd}_2 \in (0, 0.05, 0.1, \ldots 2.95, 3)$. As well, models 7−12 correspond to Eqs (4.1)−(4.6), respectively. In model 7, we add the intercept term β_0, and it has no significant effects. Both sd_1 and sd_2 have significant and positive effects on spreading duration, which implies that heterogeneity increases spreading duration under thresholds. The explanatory power (adjusted R2) is 60.06%. We drop the intercept β_0 and a much higher adjusted R2 can be achieved in models 8 to 12. Model 8 indicates that both sd_1 and sd_2 have positive effects, which means that heterogeneity enlarges the spreading process. The adjusted R2 jumps into 89.59% from 60.06%. We focus on $\text{SD} = \text{sd}_1 + \text{sd}_2$ in model 9, and SD also has positive effects on spreading duration. However, the adjusted R2 is 77.14%. The outcomes of linear effects of heterogeneity can be visualized in models 7−9. Nevertheless, there exist nonlinear effects of heterogeneity as well. In models 10−12, we introduce quadratic forms of sd_1, sd_2 and SD, to explore linear and nonlinear effects. In model 10, we estimate linear and nonlinear effects of SD, and the nonlinear effect is statistically significant. There seems to be a peak

point as the nonlinear effect of the quadratic form is negative. The adjusted R2 is about 80.35%, larger than the linear effect in model 10 (77.14%). We explore nonlinear effect of sd_1 in model 11, and its pattern is similar to the aggregate heterogeneity SD. The coefficient of the quadratic form sd_1^2 is negative, which means that there is a certain level of sd_1 that can achieve the highest spreading duration. The adjusted R2 in model 11 is also higher than merely the linear effect in model 7 (80.54% > 60.06%). We explore nonlinear effect of the sd_2, and the nonlinear effect of sd_2^2 is also negative. Under non-zero thresholds, it also postpones the duration of 100% spreading.

In Figure 8, we check the distribution of residuals for models 1−6. It suggests that the means of six residuals (blue vertical lines in the subfigures) are close to zero for most models, although some diverse values can be observed.

Table2. Linear and nonlinear effects of heterogeneity under thresholds[b].

	Model 7	Model 8	Model 9	Model 10	Model 11	Model 12
C	-12.969	/	/	/	/	/
	(8.132)					
sd_1	39.136***	36.94***	/		107.79***	
	(2.114)	(1.61)			(6.008)	
sd_1^2					-11.64***	
					(1.514)	
sd_2	37.885***	35.69***	/			112.63***
	(2.114)	(1.61)				(6.037)
sd_2^2						-12.99***
						(1.522)
$SD = (sd_1 + sd_2)$			31.363***	56.32***		
			(0.8127)	(3.019)		
$SD^2 = (sd_1 + sd_2)^2$				-3.278***		
				(0.3804)		
F-Statistics	F (2, 438)	F (2, 439)	F (1, 440)	F (2, 439)	F (2, 439)	F (2, 439)
	=331.8***	=1898***	=1489***	=902.7***	=913.6***	=902.7***
N	441	441	441	441	441	441
Adjusted R^2	0.6006	0.8959	0.7714	0.8035	0.8054	0.8035

b. * p < 0.05, ** p < 0.01, *** p < 0.001.

5. Discussions and conclusions

For the previous researches, more attention is paid to the whole process or dynamic curves [7,12,39,42,44−46,48,49,52,54,57,58,65,67], but we focus on different curves shapes. Based on specific mechanism that we found, we can better understand and predict the spreading process, according to the real target cases. Besides of two advantages, we also have two limitations. The first one is our model and setting are also ideal or simple, however real cases are also complex. The second is that some parameters and attributions of agents (netizens) are still hard to measure and calculate.

5.1. Threshold-mean effects on spreading durations

As we compare scenarios under the zero (mean) thresholds and non-zero thresholds, the effects vary with or without thresholds. Individual thresholds generally postpone the spreading process and therefore enlarge the durations. It includes: (a) As there is no threshold or the mean is zero, i.e., $\text{mean}(\text{Internal}_i) = \text{mean}(\text{External}_i) = 0$, the spreading process is much faster. In Figure 2, the mean of spreading duration is about 46.87 steps ($\text{sd}_1 = \text{sd}_2 = 0$). In Figure 3, the means are 72.34 steps ($\text{sd}_1 = \text{sd}_2 = 0.5$), 102.98 steps ($\text{sd}_1 = \text{sd}_2 = 1$), 152.5 steps ($\text{sd}_1 = \text{sd}_2 = 2$) and 220.1 steps ($\text{sd}_1 = \text{sd}_2 = 3$); (b) However, the spreading duration under non-zero thresholds, $\text{mean}(\text{Internal}_i) = \text{mean}(\text{External}_i) = 1$, is much larger. For instances, the average duration is 1678 steps in figure 4 ($\text{sd}_1 = \text{sd}_2 = 0$), 1096 steps in Figure 6A ($\text{sd}_1 = \text{sd}_2 = 0.5$), 418 steps in Figure 6B ($\text{sd}_1 = \text{sd}_2 = 1$), 267 steps in Figure 6C ($\text{sd}_1 = \text{sd}_2 = 2$), and 327 in Figure 6D ($\text{sd}_1 = \text{sd}_2 = 3$). The effect of thresholds refers to the mean of thresholds, and it plays a positive role in the spreading duration. In other words, it delays the process of rumors or information spreading. The possible reason is that thresholds mean difficulties that individuals should overcome before they spread rumors (information) to others (neighbors).

5.2. Threshold-heterogeneity (SD) effects on spreading durations

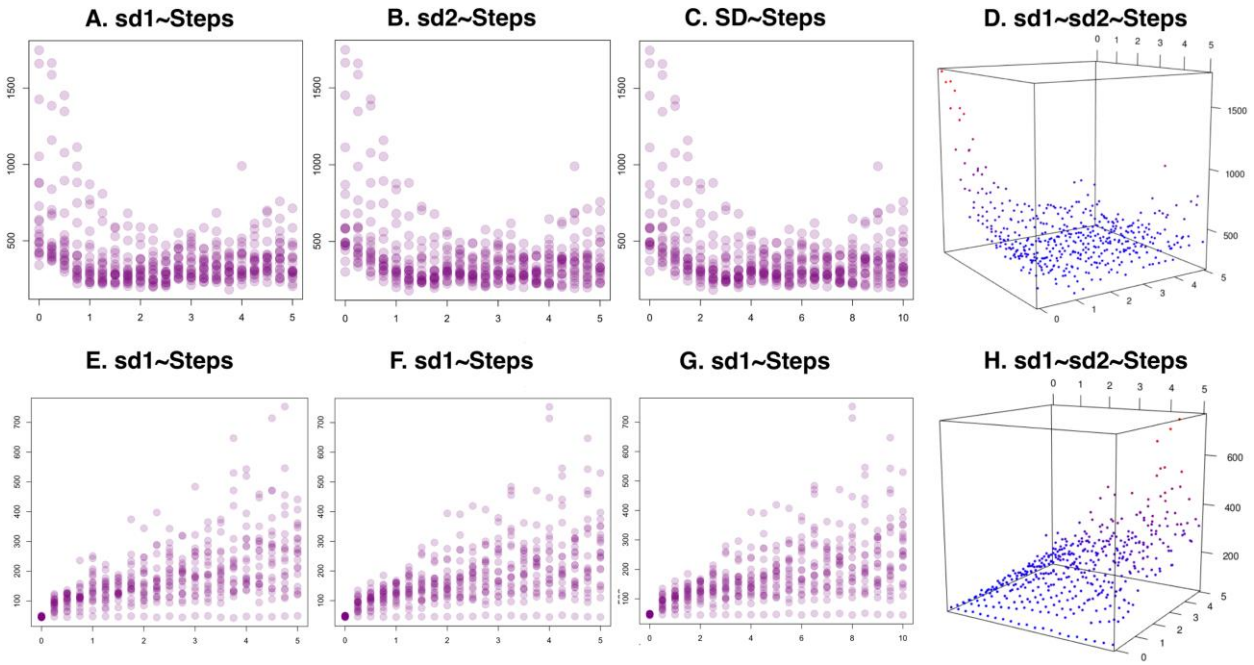

Figure 9. Visualizations of heterogeneity effects on spreading durations. Subfigures A-D refers to the zero-mean threshold situation, and subfigures E-H refers to the non-zero threshold situation. The term $\text{SD} = \text{sd1} + \text{sd2}$.

For investigating mechanisms of collective actions, the heterogeneity is the key variable, because people or agents are variant [1,3,4,7,9,13,15,27,52,70,73,74,76,100,101]. It seems that heterogeneity of individuals enhances collective behaviors [52,67,73,74,76,100−103]. However, we find that it delays or undermines the spreading process and enlarges the spreading duration. We run each simulation 300 times to compare the mean of spreading durations. In Figures 2 and 3 where the mean of threshold is zero, the heterogeneity delays the process of rumor spreading as it increases, i.e., 220.1 steps ($\mathrm{sd}_1 = \mathrm{sd}_2 = 3$) > 152.5 steps ($\mathrm{sd}_1 = \mathrm{sd}_2 = 2$) > 102.98 steps ($\mathrm{sd}_1 = \mathrm{sd}_2 = 1$) > 72.34 steps ($\mathrm{sd}_1 = \mathrm{sd}_2 = 0.5$) > 46.87 steps ($\mathrm{sd}_1 = \mathrm{sd}_2 = 0$). For zero mean threshold, Figure 9A-D shows nonlinear trends when the heterogeneity grows. Joint effects of $\mathrm{sd1}$ and $\mathrm{sd2}$ can be visualized in Figure 9D.

In Figure 6 where we have substantial thresholds, the spreading duration varies as the heterogeneity changes. It is similar that heterogeneity increases the duration and postpones the complete (100%) spreading of rumors. For instances, a weaker heterogeneity in general has shorter spreading duration in Figure 5 (homogeneity) and Figure 6 (heterogeneity), i.e., 1200 + steps ($\mathrm{sd}_1 = \mathrm{sd}_2 = 0$) > 1096 steps ($\mathrm{sd}_1 = \mathrm{sd}_2 = 0.5$) > 419 steps ($\mathrm{sd}_1 = \mathrm{sd}_2 = 1$) > 322 steps ($\mathrm{sd}_1 = \mathrm{sd}_2 = 3$) > 268 steps ($\mathrm{sd}_1 = \mathrm{sd}_2 = 2$). Therefore, heterogeneity leads to a longer spreading duration. Combining that heterogeneity improves the occurrence of collective action, it seems that heterogeneity felicitates the emergence of collective actions but results in longer durations of collective behaviors, including rumor/information spreading. For non-zero threshold, Figure 9E-H shows linear trends of spreading durations when the heterogeneity grows. The joint effects of $\mathrm{sd1}$ and $\mathrm{sd2}$ can be visualized in Figure 9H. Comparing linear trends in Figure 9E-H and nonlinear trends in Figure 9A-D, it concludes that real heterogeneity results in longer spreading durations.

5.3. Spreading curve shapes under heterogeneity

Real rumor spreading process often take on S-shape curves [6,7,13,17,18,21,24,29,36,37,39,54,55,76]. As one of the ideal types of evolutionary processes [70, 71, 72, 73, 76], we also see S-curves here: **(a) Under zero thresholds.** In Figure 2, standard S-shape curves are obtained under homogeneous zero threshold. The S-shape curves is the accumulative probability curves (CDF) of spreading percentage. For standard S-shape curves, these curves should be quite close to the CDF of normal distributions. As the CDF curve of normal distribution is given, the S-shape curve can be used to explore evolutionary dynamics or rumor spreading. Therefore, we obtain standard or ideal S-shape curves when each one has zero thresholds. As heterogeneity grows, S-shape curves have longer and longer tails. In Figure 3A ($\mathrm{sd}_1 = \mathrm{sd}_2 = 0.5$), the S-shape is almost the same as Figure 2; however, the S-shape curves in Figure 3B ($\mathrm{sd}_1 = \mathrm{sd}_2 = 1$) begin to have right tails with a tail length of about 25 steps; as the heterogeneity increases further, the length of tail is around 150 steps in Figure 3C ($\mathrm{sd}_1 = \mathrm{sd}_2 = 2$); this trend continues and the tail length is over 300 steps when $\mathrm{sd}_1 = \mathrm{sd}_2 = 3$. Given right tails removed, we also obtain typical S-shape curves; **(b) Under non-zero thresholds.** For homogeneity ($\mathrm{sd}_1 = \mathrm{sd}_2 = 0$), the curve is two-staged divided by point D. As the heterogeneity grows slightly ($\mathrm{sd}_1 = \mathrm{sd}_2 = 0.5$), the two-stage trend remains stable. However, two-stage trends become S-shape curves as heterogeneity increases further ($\mathrm{sd}_1 = \mathrm{sd}_2 \geq 1$). For instance, the curves are normal in S-shape in Figure 6B ($\mathrm{sd}_1 = \mathrm{sd}_2 = 1$). As it becomes stronger ($\mathrm{sd}_1 = \mathrm{sd}_2 \geq 2$), S-shape curves also have longer right tails.

For $sd_1 = sd_2 = 2$ the tail length is about 250 steps; for $sd_1 = sd_2 = 3$, it is over 300 steps. For under zero thresholds and under non-zero thresholds, the curves were getting more diverse under same parameter settings, as heterogeneity provides more randomness and uncertainty to the spreading process. Comparing these two situations, the S-curves can be seen when heterogeneity exists and even gets stronger. In reality, heterogeneity is inevitable [1,3,4,7,9,13,15,27,52,70,73,74,76]. Therefore, S-shape curve is the commonly-seen trends of rumor spreading. Based on the crowd detection and censoring technology [104,105], we can predict the (online) collective actions. The SIR models can also have accumulative S-shape trend [17,45,49,57,88,106], and the big difference is the mechanism. SIR models are calculated by differential equations and mathematical models not by behavior-based. To improve the investigations and predictions of online rumor-spreading, both agent-based modeling and SIR models should be combined and cross-validated. Our model can also be extended to other networks, such as complex scale-free networks. Although the intermediate process of rumor propagation in basic networks and complex scale-free networks may be different, its propagation rules and algorithm are consistent. According to specific data and network cases, we can use we can use other networks including complex scale-free networks.

Acknowledgments

This work was supported by the National Social Science Foundation of China (Grant No. 17ZDA117, 19ZDA143 & 0ASH005).

Conflict of interest

The authors declare there is no conflflict of interest.

References

1. J. Ma, D. Li, Z. Tian, Rumor spreading in online social networks by considering the bipolar social reinforcement, *Phys. A.*, **447** (2016), 108−115. https://doi.org/10.1016/j.physa.2015.12.005
2. J. Lee, Y. Choi, Informed public against false rumor in the social media era: Focusing on social media dependency, *Telemat. Inform.*, **35** (2018), 1071−1081. https://doi.org/10.1016/j.tele.2017.12.017
3. Y. Hu, Q. Pan, W. Hou, M. He, Rumor spreading model considering the proportion of wisemen in the crowd, *Phys. A.*, **505** (2018), 1084−1094. https://doi.org/10.1016/j.physa.2018.04.056
4. Q. Wang, X. Yang, W. Xi, Effects of group arguments on rumor belief and transmission in online communities: An information cascade and group polarization perspective. *Inf. Manage.*, **55** (2017), 441−449. https://doi.org/10.1016/j.im.2017.10.004
5. M. Ostilli, E. Yoneki, I. X. Leung, J. F. Mendes, P. Lió, J. Crowcroft, Statistical mechanics of rumour spreading in network communities, *Proc. Comp. Sci.*, **1** (2010), 2331−2339. https://doi.org/10.1016/j.procs.2010.04.262

6. L. Zhao, Q. Wang, J. Cheng, Y. Chen, J. Wang, W. Huang, Rumor spreading model with consideration of forgetting mechanism: A case of online blogging Live Journal, *Phys. A.*, **390** (2011), 2619−2625. https://doi.org/10.1016/j.physa.2011.03.010
7. D. Li, J. Ma, How the government's punishment and individual's sensitivity affect the rumor spreading in online social networks, *Phys. A.*, **469** (2017), 284−292. https://doi.org/10.1016/j.physa.2016.11.033
8. E. Sahafizadeh, B. T. Ladani, The impact of group propagation on rumor spreading in mobile social networks, *Phys. A.*, **506** (2018), 412−423. https://doi.org/10.1016/j.physa.2018.04.038
9. J. Ma, H. Zhu, Rumor diffusion in heterogeneous networks by considering the individuals' subjective judgment and diverse characteristics, *Phys. A.*, **499** (2018), 276−287. https://doi.org/10.1016/j.physa.2018.02.037
10. C. Pan, L. X. Yang, X. Yang, Y. Wu, Y. Y. Tang, An effective rumor-containing strategy, *Phys. A.*, **500** (2018), 80−91. https://doi.org/10.1016/j.physa.2018.02.025
11. L. Wang, G. Song, Global stability of a two-mediums rumor spreading model with media coverage, *Phys. A.*, **482** (2017), 757−771. https://doi.org/10.1016/j.physa.2017.04.027
12. N. Zhang, H. Huang, B. Su, J. Zhao, B. Zhang, Dynamic 8-state ICSAR rumor propagation model considering official rumor refutation, *Phys. A.*, **415** (2014), 333−346. https://doi.org/10.1016/j.physa.2014.07.023
13. D. Centola, The spread of behavior in an online social network experiment, *Science*, **329** (2010), 1194−1197. https://doi.org/10.1126/science.1185231
14. T. Schelling, *Micromotives and macrobehavior*, Norton Press, 2005.
15. D. M. Centola, Homophily, networks, and critical mass: Solving the start-up problem in large group collective action, *Ration. Soc.*, **25** (2013), 3−40. https://doi.org/10.1177/1043463112473734
16. M. Van Zomeren, C. W. Leach, R. Spears, Does group efficacy increase group identification? Resolving their paradoxical relationship, *J. Exp. Soc. Psychol.*, **46** (2010), 1055−1060. https://doi.org/10.1016/j.jesp.2010.05.006
17. L. Zhao, H. Cui, X. Qiu, X. Wang, J. Wang, SIR rumor spreading model in the new media age, *Phys. A.*, **392** (2013), 995−1003. https://doi.org/10.1016/j.physa.2012.09.030
18. L. Zhu, Y. Wang, Rumor diffusion model with spatio-temporal diffusion and uncertainty of behavior decision in complex social networks, *Phys. A.*, **502** (2018), 29−39. https://doi.org/10.1016/j.physa.2018.02.060
19. Y. Tanaka, Y. Sakamoto, T. Matsuka, *Transmission of rumor and criticism in twitter after the great japan earthquake*, Social Science Electronic Publishing, 2012
20. J. Shin, L. Jian, K. Driscoll, F. Bar, *Political rumoring on twitter during the 2012 us presidential election: rumor diffusion and correction*, Social Science Electronic Publishing, 2016
21. O. Oh, M. Agrawal, R. H. Rao, Community intelligence and social media services: a rumor theoretic analysis of tweets during social crises, *Mis Quart.*, **37** (2013), 407−426. https://doi.org/10.25300/misq/2013/37.2.05
22. J. Lee, M. Agrawal, H. R. Rao, Message diffusion through social network service: the case of rumor and non-rumor related tweets during boston bombing 2013, *Inform. Syst. Front.*, **17** (2015), 997−1005. https://doi.org/10.1007/s10796-015-9568-z

23. S. Hamidian, M. Diab, Rumor identification and belief investigation on Twitter, in *Proceedings of the 7th Workshop on computational approaches to subjectivity, sentiment and social media analysis*, (2016), 3−8.
24. M. Mai, A. Nadamoto, E. Aramaki, How do rumors spread during a crisis?: analysis of rumor expansion and disaffirmation on twitter after 3.11 in Japan, *Int. J. Web Inf. Syst.*, **10** (2014), 394−412. https://doi.org/10.1108/IJWIS-04-2014-0015
25. R. Escalante, M. Odehnal, A deterministic mathematical model for the spread of two rumors, *Afrika. Mat.*, **31**(2020), 315−331. https://doi.org/10.1007/s13370-019-00726-8
26. A. Y. Chua, S. Banerjee, To share or not to share: The role of epistemic belief in online health rumors, *Int. J. Med. Inform*., **108** (2017), 36−41. https://doi.org/10.1016/j.ijmedinf.2017.08.010
27. Y. Hu, Q. Pan, W. Hou, M. He, Rumor spreading model with the different attitudes towards rumors, *Phys. A.*, **502** (2018), 331−344. https://doi.org/10.1016/j.physa.2018.02.096
28. L. A. Huo, P. Huang, X. Fang, An interplay model for authorities' actions and rumor spreading in emergency event, *Phys. A.*, **390** (2011), 3267−3274. https://doi.org/10.1016/j.physa.2011.05.008
29. K. Ji, J. Liu, G. Xiang, Anti-rumor dynamics and emergence of the timing threshold on complex network, *Phys. A.*, **411** (2014), 87−94. https://doi.org/10.1016/j.physa.2014.06.013
30. W. Li, S. Tang, S. Pei, S. Yan, S. Jiang, X. Teng, et al., The rumor diffusion process with emerging independent spreaders in complex networks, *Phys. A.*, **397** (2014), 121−128. https://doi.org/10.1016/j.physa.2013.11.021
31. U. Merlone, D. Radi, Reaching consensus on rumors, *Phys. A.*, **406** (2014), 260−271. https://doi.org/10.1016/j.physa.2014.03.048
32. L. L. Xia, G. P. Jiang, B. Song, Y. R. Song, Rumor spreading model considering hesitating mechanism in complex social networks, *Phys. A.*, **437** (2015), 295−303. https://doi.org/10.1016/j.physa.2015.05.113
33. V. Giorno, S. Spina, Rumor spreading models with random denials, *Phys. A.*, **461** (2016), 569−576. https://doi.org/10.1016/j.physa.2016.06.070
34. R. Zhang, D. Li, Rumor propagation on networks with community structure, *Phys. A.*, **483** (2017), 375−385. https://doi.org/10.1016/j.physa.2017.05.006
35. L. Zhu, Y. Wang, Rumor spreading model with noise interference in complex social networks, *Phys. A.*, **469** (2017), 750−760. https://doi.org/10.1016/j.physa.2016.11.119
36. L. A. Huo, C. Ma, Dynamical analysis of rumor spreading model with impulse vaccination and time delay, *Phys. A.*, **471** (2017), 653−665. doi: 10.1016/j.physa.2016.12.024.
37. M. Jia, H. Ruan, Z. Zhang, How rumors fly, *J. Bus. Res.*, **72** (2017), 33−45. https://doi.org/10.1016/j.jbusres.2016.11.010
38. R. Y. Tian, Y. J. Liu, Isolation, insertion, and reconstruction: Three strategies to intervene in rumor spread based on super network model, *Decis. Support Syst.*, **67** (2014), 121−130. https://doi.org/10.1016/j.dss.2014.09.001
39. L. Zhao, J. Wang, Y. Chen, Q. Wang, J. Cheng, H. Cui, SIHR rumor spreading model in social networks, *Phys. A.*, **391** (2012), 2444−2453. https://doi.org/10.1016/j.physa.2011.12.008

40. L. Zhao, W. Xie, H. O. Gao, X. Qiu, X. Wang, S. Zhang, A rumor spreading model with variable forgetting rate, *Phys. A.*, **392** (2013), 6146−6154. https://doi.org/10.1016/j.physa.2013.07.080
41. L. Zhao, X. Qiu, X. Wang, J. Wang, Rumor spreading model considering forgetting and remembering mechanisms in inhomogeneous networks, *Phys. A.*, **392** (2013), 987−994. https://doi.org/10.1016/j.physa.2012.10.031
42. L. Zhao, X. Wang, X. Qiu, J. Wang, A model for the spread of rumors in Barrat-Barthelemy-Vespignani (BBV) networks, *Phys. A.*, **392** (2013), 5542−5551. https://doi.org/10.1016/j.physa.2013.07.012
43. S. Han, F. Zhuang, Q. He, Z. Shi, X. Ao, Energy model for rumor propagation on social networks, *Phys. A.*, **394** (2014), 99−109. https://doi.org/10.1016/j.physa.2013.10.003
44. K. Afassinou, Analysis of the impact of education rate on the rumor spreading mechanism, *Phys. A.*, **414** (2014), 43−52. https://doi.org/10.1016/j.physa.2014.07.041
45. J. Wang, L. Zhao, R. Huang, SIRaRu rumor spreading model in complex networks, *Phys. A.*, **398** (2014), 43−55. https://doi.org/10.1016/j.physa.2013.12.004
46. Y. Zan, J. Wu, P. Li, Q. Yu, SICR rumor spreading model in complex networks: Counterattack and self-resistance, *Phys. A.*, **405** (2014), 159−170. https://doi.org/10.1016/j.physa.2014.03.021
47. D. Li, J. Ma, Z. Tian, H. Zhu, An evolutionary game for the diffusion of rumor in complex networks, *Phys. A.*, **433** (2015), 51−58. https://doi.org/10.1016/j.physa.2015.03.080
48. R. Y. Tian, X. F. Zhang, Y. J. Liu, SSIC model: A multi-layer model for intervention of online rumors spreading, *Phys. A.*, **427** (2015), 181−191. https://doi.org/10.1016/j.physa.2015.02.008
49. Z. Qian, S. Tang, X. Zhang, Z. Zheng, The independent spreaders involved SIR rumor model in complex networks, *Phys. A.*, **429** (2015), 95−102. https://doi.org/10.1016/j.physa.2015.02.022
50. N. Song, Dynamical interplay between the dissemination of scientific knowledge and rumor spreading in emergency, *Phys. A.*, **461**(2016), 73−84. https://doi.org/10.1016/j.physa.2016.05.028
51. Z. J. Zhao, Y. M. Liu, K. X. Wang, An analysis of rumor propagation based on propagation force, *Phys. A.*, **443** (2016), 263−271. https://doi.org/10.1016/j.physa.2015.09.060
52. R. Jie, J. Qiao, G. Xu, Y. Meng, A study on the interaction between two rumors in homogeneous complex networks under symmetric conditions, *Phys. A.*, **454** (2016), 129−142. https://doi.org/10.1016/j.physa.2016.02.048
53. S. Hosseini, M. A. Azgomi, A model for malware propagation in scale-free networks based on rumor spreading process. *Comput. Netw.*, **108** (2016), 97−107. doi: 10.1016/j.comnet.2016.08.010
54. X. Qiu, L. Zhao, J. Wang, X. Wang, Q. Wang, Effects of time-dependent diffusion behaviors on the rumor spreading in social networks. *Phys. Lett. A*, **380** (2016), 2054−2063. https://doi.org/10.1016/j.physleta.2016.04.025
55. Q. Liu, T. Li, M. Sun, The analysis of an SEIR rumor propagation model on heterogeneous network, *Phys. A.*, **469** (2017), 372−380. https://doi.org/10.1016/j.physa.2016.11.067

56. Y. Zhang, Y. Su, L. Weigang, , H. Liu, Rumor and authoritative information propagation model considering super spreading in complex social networks, *Phys. A.*, **506** (2018), 395−411. https://doi.org/10.1016/j.physa.2018.04.082
57. Y. Zan, DSIR double-rumors spreading model in complex networks, *Phys. A.*, **110** (2018), 191−202. https://doi.org/10.1016/j.chaos.2018.03.021
58. Y. Cheng, C. Liu, F. Ding, Dynamic analysis of rumor spreading model for considering active network nodes and nonlinear spreading rate, *Phys. A.*, **506** (2018), 24−35. https://doi.org/10.1016/j.physa.2018.03.063
59. O. Oh, P. Gupta, M. Agrawal, H. R. Rao, ICT mediated rumor beliefs and resulting user actions during a community crisis, *Gov. Inform. Q.*, **35** (2018), 243−258. https://doi.org/10.1016/j.giq.2018.03.006
60. W. Chen, Y. Zhang, C. K. Yeo, C. T. Lau, B. S. Lee, Unsupervised rumor detection based on users' behaviors using neural networks, *Pattern Recogn. Lett.*, **105** (2017), 226−233. https://doi.org/10.1016/j.patrec.2017.10.014
61. F. Jia, G. Lv, Dynamic analysis of a stochastic rumor propagation model, *Phys. A.*, **490** (2018), 613−623. https://doi.org/10.1016/j.physa.2017.08.125
62. J. Jia, W. Wu, A rumor transmission model with incubation in social networks, *Phys. A.*, **491** (2018), 453−462. https://doi.org/10.1016/j.physa.2017.09.063
63. H. L. Liu, C. Ma, B. B. Xiang, M. Tang, H. F. Zhang, Identifying multiple influential spreaders based on generalized closeness centrality, *Phys. A.*, **492** (2018), 2237−2248. https://doi.org/10.1016/j.physa.2017.11.138
64. Y. Zhang, J. Zhu, Stability analysis of I2S2R rumor spreading model in complex networks, *Phys. A.*, **503** (2018), 862−881. https://doi.org/10.1016/j.physa.2018.02.087
65. S. Dong, F. H. Fan, Y. C. Huang, Studies on the population dynamics of a rumor-spreading model in online social networks, *Phys. A.*, **492** (2018), 10−20. https://doi.org/10.1016/j.physa.2017.09.077
66. A. Zubiaga, E. Kochkina, M. Liakata, R. Procter, M. Lukasik, K. Bontcheva, et al., Discourse-aware rumour stance classification in social media using sequential classifiers, *Inf. Process. Manage.*, **54** (2018), 273−290. https://doi.org/10.1016/j.ipm.2017.11.009
67. J. Wang, L. Zhao, R. Huang, 2SI2R rumor spreading model in homogeneous networks, *Phys. A.*, **413** (2014), 153−161. https://doi.org/10.1016/j.physa.2014.06.053
68. R. Escalante, M. Odehnal,. Prediction of trending topics using ANFIS and deterministic models, preprint, arxiv: 1709.07535.
69. S. Tarrow, National politics and collective action: Recent theory and research in Western Europe and the United States, *Annu. Rev. Sociol.*, **14** (1988), 421−440. doi: 10.1146/annurev.so.14.080188.002225
70. X. Zhao, J. Wang, Dynamical model about rumor spreading with medium, *Discrete Dyn. Nat. Soc.*, **2013** (2013). https://doi.org/10.1155/2013/586867
71. D. Trpevski, W. K. Tang, L. Kocarev, Model for rumor spreading over networks. *Phys. Rev. E Stat. Nonlinear Soft Matter Phys*., **81** (2010), 056102. https://doi.org/10.1103/PhysRevE.81.056102

72. W. Ruigrok, W. Amann, H. Wagner, The internationalization-performance relationship at swiss firms: a test of the s-shape and extreme degrees of internationalization, *Manage. Int. Rev.*, **47** (2007), 349−368. https://doi.org/10.1007/s11575-007-0020-6
73. A. Flache, M. W. Macy, Stochastic collusion and the power law of learning: a general reinforcement learning model of cooperation, *J. Conflict Resolut.*, **46** (2002), 629−653. https://doi.org/10.1177/002200202236167
74. M. W. Macy, Learning theory and the logic of critical mass, *Am. Sociol. Rev*., **55** (1990), 809−826. https://doi.org/10.2307/2095747
75. Y. H. Guan, L. Lv, R. Duan, Y. H. Ji, The brain image segmentation by markov field and normal distribution curve, in *International Congress on Image and Signal Processing*, *IEEE*, (2009), 1−5. https://doi.org/10.1109/CISP.2009.5303479
76. M. Granovetter, Threshold models of collective behavior, *Am. J. Sociol*., **83** (1978), 1420−1443.
77. H. J. Li, L. Wang, Multi-scale asynchronous belief percolation model on multiplex networks, *New J. Phys.*, **21** (2019).
78. Z. L. Hu, L. Wang, C. B. Tang, Locating the source node of diffusion process in cyber-physical networks via minimum observers, Chaos An Interdiscip. *J. Nonlinear Sci*., **29** (2019), 063117. https://doi.org/10.1063/1.5092772
79. L. Wang, J. T. Wu, Characterizing the dynamics underlying global spread of epidemics, *Nat. Commun.*, **9** (2018), 1−11. https://doi.org/10.1038/s41467-017-02344-z
80. J. Wang, L.Wang, X. Li, Identifying spatial invasion of pandemics on metapopulation networks via anatomizing arrival history, *IEEE T. Cybernetics*, **46** (2015), 2782−2795. https://doi.org/10.1109/tcyb.2015.2489702
81. Z. Wang, L. Wang, A. Szolnoki, M. Perc, Evolutionary games on multilayer networks: a colloquium, *Eur. Phys. J. B.*, **88** (2015), 1−15. https://doi.org/10.1140/epjb/e2015-60270-7
82. Z. Wang, D. W. Zhao, L. Wang, G. Q. Sun, Z. Jin, Immunity of multiplex networks via acquaintance vaccination, *Epl*, **112** (2015), 6. https://doi.org/10.1209/0295-5075/112/48002
83. D. He, R. Lui, L. Wang, C. K. Tse, L.Yang, L. Stone, Global spatio-temporal patterns of influenza in the post-pandemic era, *Sci. Rep*., **5** (2015), 11013. https://doi.org/10.1038/srep11013
84. Z.Wang, M. A. Andrews, Z. X. Wu, L. Wang, C. T. Bauch, Coupled disease-behavior dynamics on complex networks: A review, *Phys. Life Rev.*, **15** (2015), 1−29. https://doi.org/10.1016/j.plrev.2015.07.006
85. D. Zhao, L.Wang, S. Li, Z. Wang, L. Wang, B. Gao, Immunization of epidemics in multiplex networks, *Plos One*, **9** (2014). https://doi.org/10.1371/journal.pone.0112018
86. L. Wang, X. Li, Spatial epidemiology of networked metapopulation: an overview, *Chin. Sci. Bull*., **59** (2014), 3511−3522. https://doi.org/10.1007/s11434-014-0499-8
87. Z. Wang, Y. Liu, L. Wang, Y. Zhang, Z. Wang, Freezing period strongly impacts the emergence of a global consensus in the voter model, *Sci. Rep*., **4** (2014). https://doi.org/10.1038/srep03597
88. L. Wang, Y. Zhang, Z. Wang, X. Li, The impact of human location-specific contact pattern on the sir epidemic transmission between populations, *Int. J. Bifurcat. Chaos*, **23** (2013). https://doi.org/10.1142/s0218127413500958

89. L. Wang, Z. Wang, Y. Zhang, X. Li, How human location-specific contact patterns impact spatial transmission between populations?, *Sci. Rep*., **3** (2013), 1−10. https://doi.org/10.1038/srep01468
90. H. F. Zhang, Z. X. Wu, X. K. Xu, M. Small, L. Wang, B. H. Wang, Impacts of subsidy policies on vaccination decisions in contact networks, *Phys. Rev. E*, **88** (2013). https://doi.org/10.1103/PhysRevE.88.012813
91. G. Q. Zhang, Q. B. Sun, L. Wang, Noise-induced enhancement of network reciprocity in social dilemmas. *Chaos Solitons Fractals*, **51** (2013), 31−35. https://doi.org/10.1016/j.chaos.2013.03.003
92. L. Wang, Y. Zhang, T. Y. Huang, X. Li, Estimating the value of containment strategies in delaying the arrival time of an influenza pandemic: A case study of travel restriction and patient isolatio, *Phys. Rev. E*, **86** (2012), 5. https://doi.org/10.1103/PhysRevE.86.032901
93. Y. Zhang, L.Wang, Y. Q. Zhang, X. Li, Towards a temporal network analysis of interactive WiFi users, *Epl*, **98**(2012), 6. https://doi.org/10.1209/0295-5075/98/68002
94. L. Wang, X. Li, Y. Q. Zhang, Y. Zhang, K. Zhang, Evolution of scaling emergence in large-scale spatial epidemic spreading, Plos One, **6** (2011), 11. https://doi.org/10.1371/journal.pone.0021197
95. Y. Q. Wang, X. Y. Yang, Y. L. Han, X. A. Wang, Rumor spreading model with trust mechanism in complex social networks, *Commun. Theor. Phys*., **59** (2013), 510−516. https://doi.org/10.1088/0253-6102/59/4/21
96. H. Huang, A war of (mis) information: The political effects of rumors and rumor rebuttals in an authoritarian country, *Brit. J Polit. Sci*., **47** (2017), 283−311. https://doi.org/10.1017/S0007123415000253
97. A. J. Berinsky, Rumors and health care reform: experiments in political misinformation, *Brit. J. Polit. Sci*., **47** (2017), 241−262. https://doi.org/10.1017/s0007123415000186
98. S. Tisue, U. Wilensky, NetLogo: Design and implementation of a multi-agent modeling environment, *Proc. Agent*, **2004** (2004), 7−9
99. U. Wilensky, W. Rand, *An introduction to agent-based modeling: modeling natural, social, and engineered complex systems with NetLogo*, Mit Press, 2015.
100. Q. Wang, H. Wang, Z. Zhang, Y. Li, Y. Liu, M. Perc, Heterogeneous investments promote cooperation in evolutionary public goods games, *Phys. A.*, **502** (2018), 570−575. https://doi.org/10.1016/j.physa.2018.02.140
101. M. A. Amaral, L. Wardil, M. Perc, J. K. L. D. Silva, Evolutionary mixed games in structured populations: cooperation and the benefits of heterogeneity, *Phys. Rev. E*, **93** (2016), 042304. https://doi.org/10.1103/PhysRevE.93.042304
102. M. Perc, Does strong heterogeneity promote cooperation by group interactions?, *New J. Phys*., **13** (2011), 123027−123037. https://doi.org/10.1088/1367-2630/13/12/123027
103. Z. Wang, Heterogeneous aspirations promote cooperation in the prisoner's dilemma game, *Plos One*, **5** (2010), e15117. https://doi.org/10.1371/journal.pone.0015117
104. V. Mahadevan, W. Li, V. Bhalodia, N. Vasconcelos, Anomaly detection in crowded scenes, in *2010 IEEE Computer Society Conference on Computer Vision and Pattern Recognition*, 2010. https://doi.org/10.1109/CVPR.2010.5539872

105. T. Wang, Z. Miao, Yuxin Chen, Y. Zhou, G. C. Shan, H. Snoussi., AED-net: An abnormal event detection network, *Engineering*, **5** (2019), 930−939. https://doi.org10.1016/j.eng.2019.02.008